

# Triple-layer nanostructured WO<sub>3</sub> photoanodes with enhanced photocurrent generation and superior stability for photoelectrochemical solar energy conversion

Huan Qi,<sup>a</sup> Jonathan Wolfe,<sup>b</sup> Danping Wang,<sup>c</sup> Hong Jin Fan,<sup>c</sup> Denis Fichou<sup>\*c,d</sup> and Zhong Chen<sup>\*a,e</sup>

<sup>a</sup> School of Materials Science Engineering, Nanyang Technological University, Singapore 639798, Singapore. Tel: +65 67904256; E-mail: [aszchen@ntu.edu.sg](mailto:aszchen@ntu.edu.sg)

<sup>b</sup> Interdisciplinary Graduate School, Nanyang Technological University, Singapore 639798, Singapore.

<sup>c</sup> School of Physical and Mathematical Sciences, Nanyang Technological University, 637371, Singapore.

<sup>d</sup> Sorbonne Universités, UPMC Univ Paris 06, UMR 8232, Institut Parisien de Chimie Moléculaire, F-75005, Paris, France. Tel: +33 144275080; E-mail: [denis.fichou@upmc.fr](mailto:denis.fichou@upmc.fr);

<sup>e</sup> Energy Research Institute at NTU (ERI@N), 1 CleanTech Loop, #06-04, CleanTech One, Singapore 6371412

## Electronic Supporting Information (ESI)

<b>Experimental</b>	<b>Page</b>
<i>Fabrication of WO<sub>3</sub> triple-layers</i>	2
<i>WO<sub>3</sub> triple-layer characterizations</i>	2
<i>Photoelectrochemical (PEC) measurements</i>	2
<i>Electrochemical impedance spectroscopy (EIS)</i>	3
<i>Incident photon-to-current efficiency (IPCE)</i>	3
<b>Results</b>	
<i>Cross sectional FESEM micrograph of triple layer WO<sub>3</sub> film</i>	4
<i>Atomic force microscopy (AFM)</i>	4
<i>UV-visible reflectance and (b) photoluminescence</i>	5
<i>TEM images of WO<sub>3</sub> nanoparticles NPs and nanorods NRs</i>	6
<i>FESEM micrograph of a single layer WO<sub>3</sub> film</i>	6
<i>LSV curves of hydrothermal single layer and anodized triple layer</i>	6
<i>IPCE of a WO<sub>3</sub> triple layer</i>	7
<i>Mott Schottky plots of a WO<sub>3</sub> triple layer</i>	7
<i>Energy diagram of a WO<sub>3</sub> triple layer</i>	8

## Experimental

### *Fabrication of WO<sub>3</sub> triple-layers*

Anodization of the tungsten foils was carried out by applying 30 V between a platinum cathode and a 2×2 cm<sup>2</sup> metallic tungsten foil (GoodFellow, 99.95%, 0.2 mm) in an acidic electrolyte made of 25 ml 1.5M HNO<sub>3</sub> and 40 mg NH<sub>4</sub>F. The anodization time was precisely controlled and set to be in the range 1-4 hours, resulting in WO<sub>3</sub> overlayers of increasing thicknesses in the range 1.4-3.0 μm. During anodization, the electrolyte temperature was maintained at 50°C. After anodization, samples were washed carefully with distilled water and dried by a nitrogen gas flow, followed by annealing in air at 550°C during 4 hours. A 10 nm-thick TiO<sub>2</sub> layer was finally deposited on selected samples by atomic layer deposition (ALD, Beneq TFS 200) using TiCl<sub>4</sub> and H<sub>2</sub>O as the precursors.

Hydrothermal samples were prepared using the same tungsten foil. The cleaned tungsten foil was immersed into 25ml 1.5M HNO<sub>3</sub> solution containing 40mg NH<sub>4</sub>F, in a Teflon autoclave reactor, heated at 120°C for 6 hours, followed by annealing in air at 550°C for 4 hours.

### *WO<sub>3</sub> triple-layer characterizations*

The crystal phase of the WO<sub>3</sub> overlayers was studied using a Shimadzu thin film X-ray diffractometer with a Cu Ka excitation ( $\lambda=1.54 \text{ \AA}$ ). Microscopic morphologies including lattice analysis of scraped particles were obtained using field emission scanning electron microscopy (FESEM, JEOL JSM-7600F) and high resolution transmission electron microscopy (HRTEM, JEOL-2100F) operating at 200 kV. Optical reflectance spectra of the WO<sub>3</sub> films were measured by a Shimadzu 2550 UV-visible-NIR spectrophotometer with a reflectance detection angle of 5°. Photoluminescence (PL) spectra were recorded on a fluorescence spectrophotometer (Varian Cary Eclipse) at room temperature with an excitation wavelength of 300 nm.

### *Photoelectrochemical (PEC) measurements*

All measurements were conducted in a 0.5M H<sub>2</sub>SO<sub>4</sub> electrolyte using a three-electrode configuration with a WO<sub>3</sub> working electrode and Pt and Ag/AgCl electrodes as counter and reference electrodes, respectively. The inter-electrode spacing was ≈1 cm. Photocurrents were recorded using PCI4/300™ potentiostat with PHE200™ software (Gamry

Instruments, Inc.). The working  $\text{WO}_3$  electrodes were exposed to the light of a solar simulator equipped with a 300 W Xe-lamp (HAL-320, Asahi Spectra Co., Ltd.). The incident light intensity was  $100 \text{ mW}\cdot\text{cm}^{-2}$  and the sample illumination area  $0.76 \text{ cm}^2$ . Linear sweep voltammetry (LSV) was carried out under both dark and illumination conditions with a scan rate of  $10 \text{ mV}\cdot\text{s}^{-1}$  with chopped light irradiation (frequency=0.2 Hz). Stability tests were conducted by chronoamperometry under a potential of  $0.8 \text{ V vs RHE}$  in a pH=7 buffer solution, with periodic light on/off cycles of 50 seconds duration every 50 seconds.

#### *Electrochemical impedance spectroscopy (EIS)*

Electrochemical impedance spectroscopy (EIS) was conducted in the same configuration using PCI4/300™ potentiostat with EIS300™ software (Gamry Instruments, Inc.). Potentiostatic mode was applied under illumination conditions, at an applied voltage of  $1 \text{ V vs. RHE}$ . AC perturbations of amplitude 5 mV were superimposed with frequency ranging from 0.01 Hz to 100 kHz. Equivalent circuit modeling and curve fitting were performed using the Echem Analyst™ software (Gamry Instruments, Inc.).

#### *Incident photon-to-current efficiency (IPCE)*

IPCE of samples were measured with a xenon light source (Asahi Spectra Co. Ltd.) together with a monochromator (Asahi Spectra Co. Ltd.) from 350 nm to 550 nm, at potentials of  $1.0 \text{ V vs RHE}$ , combined with silicon photodiode (Bentham, DH-Si) with known IPCE value.

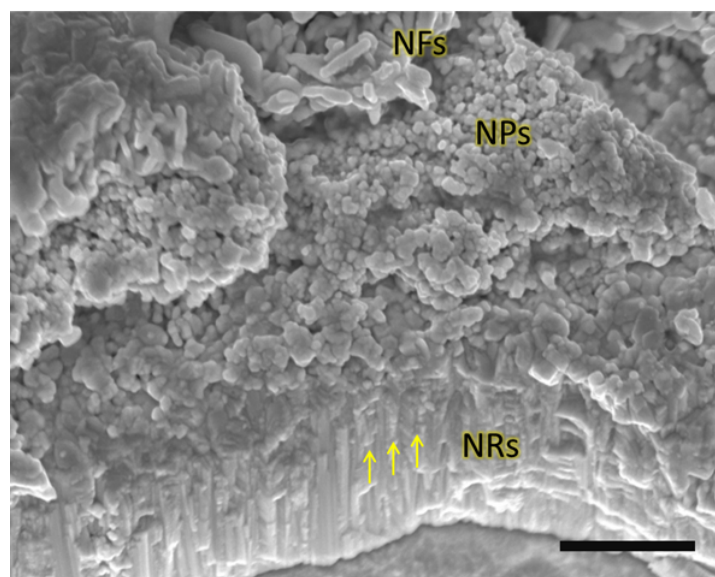


**Fig. S1** FESEM image of the triple-layered  $\text{WO}_3$ . The scale bar is 1  $\mu\text{m}$ .

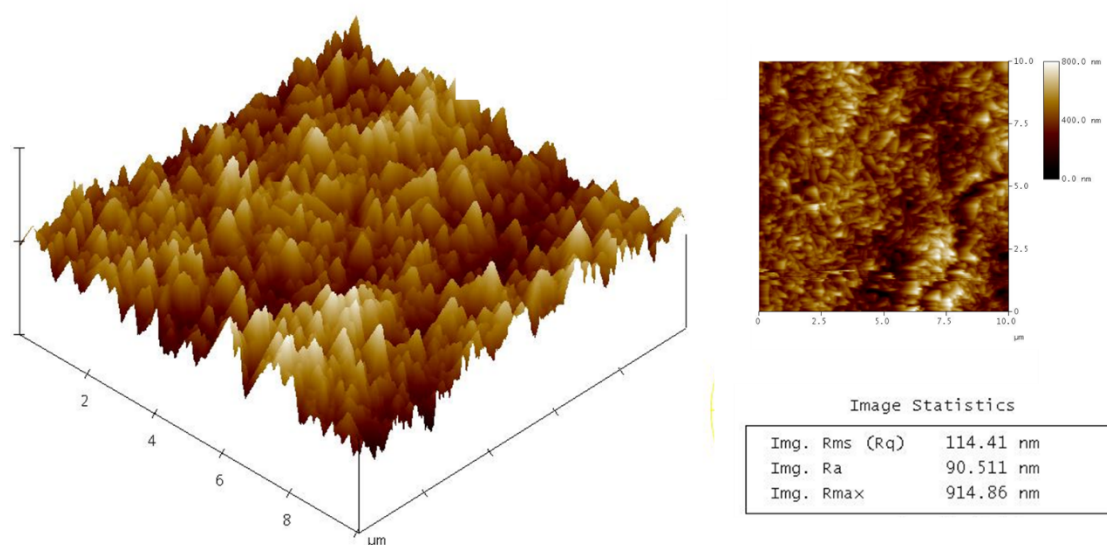


**Fig. S2** Atomic force microscopy (AFM) of a tungsten foil after an anodization time of 4 hours.

The surface roughness and the surface morphology of the triple-layer  $\text{WO}_3$  thin film were analyzed by the atomic force microscopy DI-3100. The mode working was tapping mode through the use of probe in a radius of 15nm. From the AFM image, Surface roughness  $R_{\text{ms}}$  value of 114.41 nm is calculated. This roughness provides a large surface area, thus improving considerably light absorption of  $\text{WO}_3$  photoanodes.

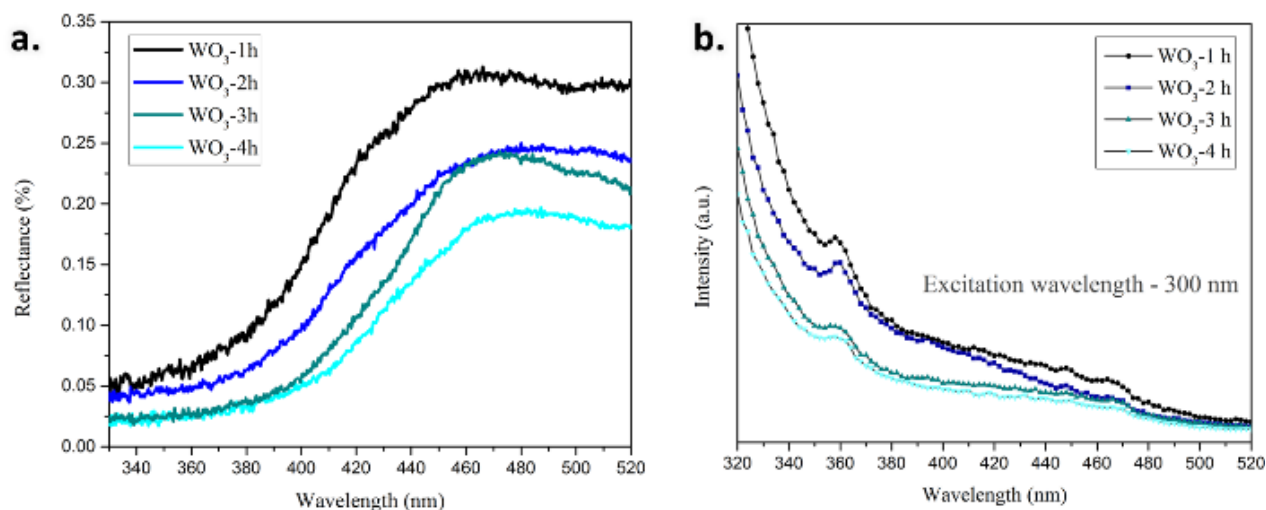


**Fig. S3** (a) UV-visible reflectance and (b) photoluminescence ( $\lambda_{\text{ex}}=300$  nm) spectra of  $\text{WO}_3$  after anodization during 1h, 2h, 3h and 4h respectively.

UV-visible optical absorption and photoluminescence (PL) were used to further investigate the light harvesting capability of  $\text{WO}_3$  triple layers. After anodization times of 1-4 hours the PL spectra show no peak shift.

$\text{WO}_3$  is an indirect bandgap semiconductor, of which the electron-hole recombination loss is only through photon emission or absorption for the wave vector compensation<sup>1</sup>. The photon emission is measured through photoluminescence spectra, which is corresponding to the electron-hole recombination efficiency. With different excitation wavelength, the peak position can be varied. In this case, under 300 nm as excitation light, there are two peaks observed in 360 nm and 465 nm, of which 465 nm is corresponding to the band gap value measured. While for 360 nm shorter UV emission observed may come from the quantum-confinement-effect on the band gap<sup>1</sup>. Both peaks decrease in intensity with increasing anodization time up to 4 hours, thus indicating an improved charge separation induced by the nanostructured NR/NP/NF triple-layer.

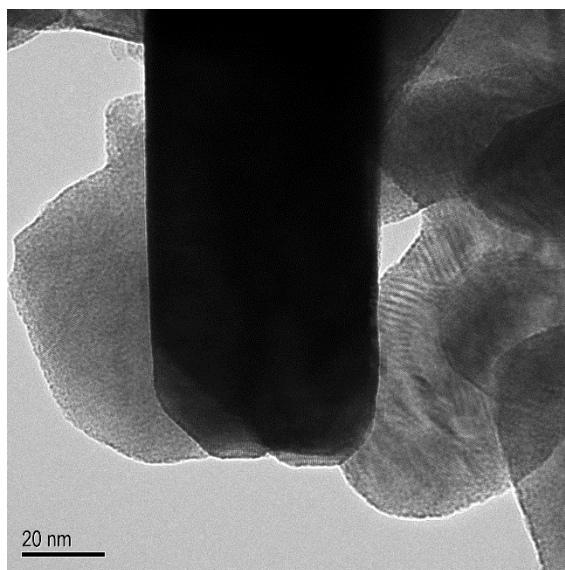


**Fig. S4** TEM images of  $\text{WO}_3$  nanoparticles NPs (dark) and nanorods NRs (light).

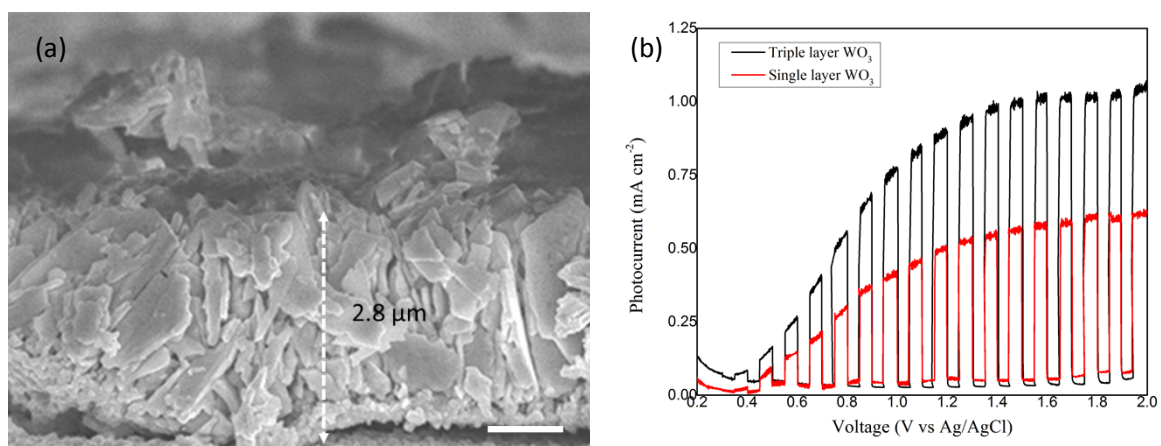


**Fig. S5** (a) FESEM micrograph of a single layer  $\text{WO}_3$  film (thickness 2.8  $\mu\text{m}$ ) prepared by the hydrothermal method, the scale bar is 1  $\mu\text{m}$ . (b) Respective linear sweep voltammograms of hydrothermal single layer (red) and anodized triple layer (black) performed on samples having similar thickness.

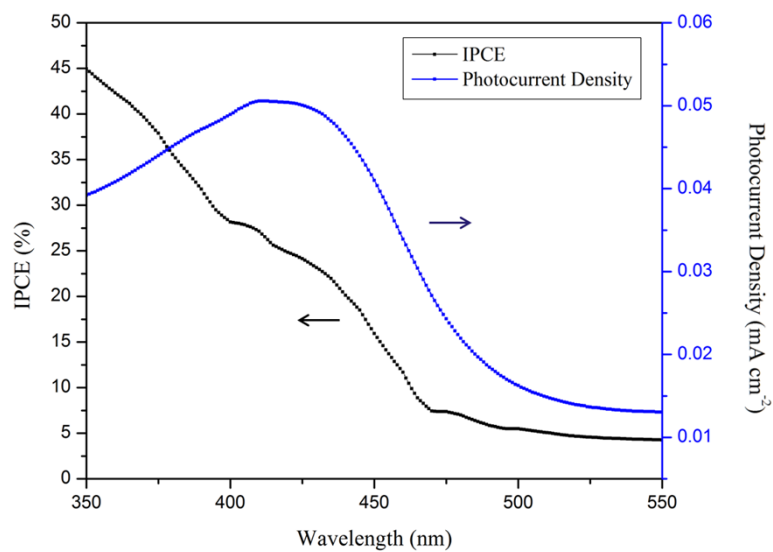


**Fig. S6** IPCE of WO<sub>3</sub> triple layer after an anodization time of 4 hours.

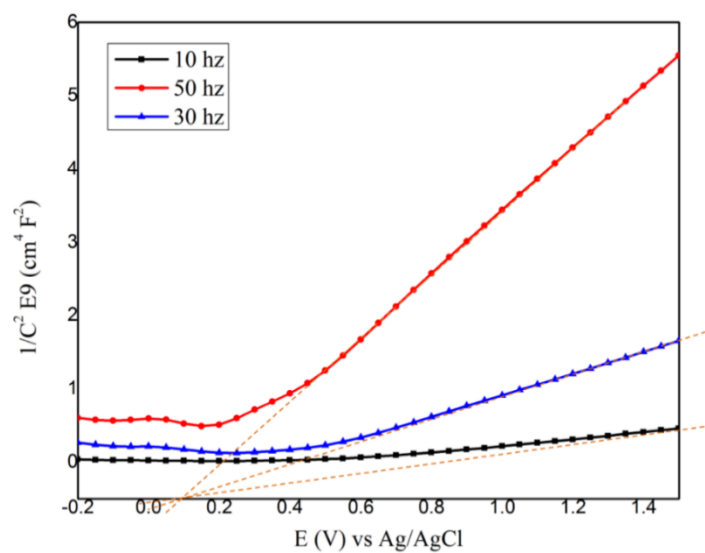


**Fig. S7** Mott-Schottky plots of a WO<sub>3</sub> triple layer after an anodization time of 4 hours in 1M HCl at AC amplitude of 10 Hz, 30 Hz and 50 Hz.

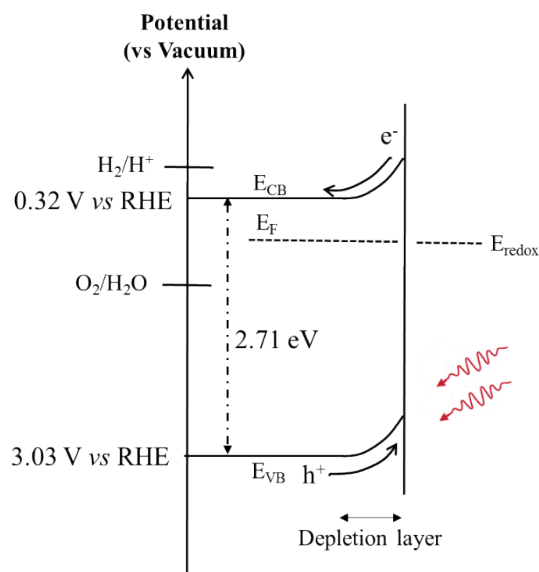


**Fig. S8** Energy diagram of  $\text{WO}_3$  triple layer after an anodization time of 4 hours.

From the Mott-Schottky plots in Fig. S6, a flat-band potential for the  $\text{WO}_3$  film of  $V_{\text{fb}}=0.32$  V vs RHE is obtained. Combined with a band-gap value of 2.71 eV obtained from the UV-visible reflectance spectra, the band position of as-synthesized  $\text{WO}_3$  can be calculated, as shown in Fig. S7. The valence band energy level of 3.03 V vs RHE clearly shows that the  $\text{WO}_3$  triple-layers can be used as efficient photoanodes for water splitting applications.

## References

- [1] M. Feng, A. L. Pan, H. R. Zhang, Z. A. Li, F. Liu, H. W. Liu, D. X. Shi, B. S. Zou, and H. J. Gao, *Applied Physics Letters*, 2005, **86**, 141901